

Optimal synchronization of higher-order Kuramoto model on hypergraphs

Chong-Yang Wang(王重阳), Bi-Yun Ji(季碧芸), Linyuan Lü(吕琳媛)
Citation: Chin. Phys. B, 2025, 34 (**7**): 070502. DOI: 10.1088/1674-1056/adcded
Journal homepage: http://cpb.iphy.ac.cn; http://iopscience.iop.org/cpb

What follows is a list of articles you may be interested in

Associated network family of the unified piecewise linear chaotic family and their relevance

Haoying Niu(牛浩瀛) and Jie Liu(刘杰)
Chin. Phys. B, 2025, 34 (**4**): 040503. DOI: 10.1088/1674-1056/adb26a、

Detection of EEG signals in normal and epileptic seizures with multiscale multifractal analysis approach via weighted horizontal visibility graph

Lu Ma(马璐), Yan-Lin Ren(任彦霖), Ai-Jun He(何爱军), De-Qiang Cheng(程德强), and Xiao-Dong Yang(杨小冬)
Chin. Phys. B, 2023, 32 (**11**): 110506. DOI: 10.1088/1674-1056/acdfbf

Explosive synchronization of multi-layer complex networks based on star connection between layers with delay

Yan-Liang Jin(金彦亮), Qian-Yuan Han(韩钱源), Run-Zhu Guo(郭润珠), Yuan Gao(高塬), and Li-Quan Shen(沈礼权)
Chin. Phys. B, 2023, 32 (**10**): 100507. DOI: 10.1088/1674-1056/acbaf1

Stability and multistability of synchronization in networks of coupled phase oscillators

Yun Zhai(翟云), Xuan Wang(王璇), Jinghua Xiao(肖井华), and Zhigang Zheng(郑志刚)
Chin. Phys. B, 2023, 32 (**6**): 060503. DOI: 10.1088/1674-1056/acc808

Synchronization of stochastic complex networks with time-delayed coupling

Duolan(朵兰), Linying Xiang(项林英), and Guanrong Chen(陈关荣)
Chin. Phys. B, 2023, 32 (**6**): 060502. DOI: 10.1088/1674-1056/acc44e

---

Optimal synchronization of higher-order Kuramoto model on hypergraphs

Chong-Yang Wang(王重阳)[1,2,3,†], Bi-Yun Ji(季碧芸)[1,2], and Linyuan Lü(吕琳媛)[4,‡]

[1] *Yangtze Delta Region Institute of University of Electronic Science and Technology of China, Huzhou* 313000, *China*
[2] *Institute of Fundamental and Frontier Sciences, University of Electronic Science and Technology of China, Chengdu* 611731, *China*
[3] *Lanzhou Center for Theoretical Physics, Key Laboratory of Theoretical Physics of Gansu Province, and Key Laboratory of Quantum Theory and Applications of Ministry of Education, Lanzhou University, Lanzhou* 730000, *China*
[4] *School of Cyber Science and Technology, University of Science and Technology of China, Hefei* 230026, *China*

(Received 10 February 2025; revised manuscript received 8 April 2025; accepted manuscript online 17 April 2025)

Complex networks play a crucial role in the study of collective behavior, encompassing the analysis of dynamical properties and network topology. In real-world systems, higher-order interactions among multiple entities are widespread and significantly influence collective dynamics. Here, we extend the synchronization alignment function framework to hypergraphs of arbitrary order by leveraging the multi-order Laplacian matrix to encode higher-order interactions. Our findings reveal that the upper bound of synchronous behavior is determined by the maximum eigenvalue of the multi-order Laplacian matrix. Furthermore, we decompose the contribution of each hyperedge to this eigenvalue and utilize it as a basis for designing an eigenvalue-based topology modification algorithm. This algorithm effectively enhances the upper bound of synchronous behavior without altering the total number of higher-order interactions. Our study provides new insights into dynamical optimization and topology tuning in hypergraphs, advancing the understanding of the interplay between higher-order interactions and collective dynamics.

Keywords: synchronization optimization, hypergraph, complex network

PACS: 05.45.Xt, 05.10.–a, 64.60.aq

DOI: 10.1088/1674-1056/adcded **CSTR:** 32038.14.CPB.adcded

1. Introduction

Collective behaviors, especially synchronization phenomena, are prevalent in a wide range of fields, including nature,[1–3] society,[4,5] engineering technologies,[6–8] and so on. These behaviors can be analyzed through network science from the perspective of the relationship between dynamics and network structure, which provides a structural foundation for analyzing dynamic processes across disciplines due to its flexibility and broad applicability.[9–22] Beyond the typical pairwise interactions used to characterize the communication between individuals, numerous studies have demonstrated that many real-world systems exhibit patterns of higher-order interactions,[23–28] which are often modeled as simplicial complexes or hypergraphs to capture the architecture of complex systems.[19–22] With these effective representations of higher-order networks, various higher-order Kuramoto models have been proposed to explore the synchronous behavior of complex systems with higher-order interactions, providing critical new insights into the dynamical processes.[23–28] Although some studies have examined the role of higher-order interactions in the synchronous behavior of heterogeneous systems,[29–32] they have primarily focused on simplex networks, while real-world systems often involve more intricate interactions.

The study of synchronization on complex networks encompasses not only analyzing the dynamical properties of the system from the perspective of network topology, but also investigating how to achieve optimal synchronization.[33] On the one hand, for a fixed network structure, the optimal synchronization of a system can be achieved by adjusting individual characteristics.[34,35] Skardal *et al.*[35] studied the optimization of collective behavior in networks with higher-order interactions encoded in clique complexes. They adapted the synchrony alignment function framework to a composite Laplacian matrix that encodes multi-order interactions and demonstrated that higher-order interactions can better optimize network synchronization. However, the optimization effects of more general higher-order interactions (e.g., hypergraphs) on collective dynamics remain insufficiently understood.

On the other hand, a more straightforward approach to achieve optimal synchronization is to design the best network architecture.[12,13] The underlying structure of a network plays a pivotal role in determining its synchronization capability.[36–39] Nowadays, most efforts to optimize network topology have primarily been limited to networks with pairwise interactions[40–42] or to stochastic reconnection

†Corresponding author. E-mail: wangchongyang@csj.uestc.edu.cn
‡Corresponding author. E-mail: linyuan.lv@uestc.edu.cn

© 2025 Chinese Physical Society and IOP Publishing Ltd. All rights, including for text and data mining, AI training, and similar technologies, are reserved.

methods.[43] The relationship between the interaction mode, structural features, and synchronization behavior remains incompletely elucidated. Therefore, another critical question in the optimization of collective behavior is to identify or design topologies or features that are more conducive to synchronization optimization, and how synchronization performance can be enhanced through topology modification.

In this study, we investigate the collective dynamics of synchronization on hypergraphs, with a particular focus on optimal synchronization and network topology. We introduce a multi-order Laplacian matrix applicable to arbitrary hypergraphs, which encapsulates higher-order collective dynamics under strong synchronization constraints and quantifies the optimal collective behavior allowed by a given network topology with higher-order interactions. Furthermore, we extend the synchronization alignment function (SAF) framework[34] from simplicial complexes to hypergraphs and establish that the upper bound of synchronous behavior in a hypergraph is determined by the maximum eigenvalue of the multi-order Laplacian matrix. Additionally, we decompose the contribution to the maximum eigenvalue from individual hyperedges and, building on this analysis, propose an eigenvalue-based hypergraph topology modification method. This approach effectively optimizes the eigenvalues of the multi-order Laplacian matrix, thereby enhancing the upper bound of synchronous behavior while preserving the number of higher-order interactions.

Our findings contribute to a deeper theoretical understanding of the intricate relationship between network topology and synchronous behavior, and provide a foundation for future research on controlling and optimizing dynamical processes in systems with higher-order interactions.

2. Higher-order Kuramoto model

We begin with a generalized higher-order Kuramoto model with a population of N oscillators on a hypergraph, incorporating many-body interactions with any order $d = 1,2,\ldots,D$, whose dynamics are governed by[44]

$$\begin{aligned}\dot{\theta}_i = {} & \omega_i + \frac{K_1}{\langle k^{(1)}\rangle}\sum_{j=1}^{N} M_{ij}^{(1)}\sin(\theta_j-\theta_i) \\ & + \frac{K_2}{2!\langle k^{(2)}\rangle}\sum_{j_1,j_2=1}^{N} M_{ij_1j_2}^{(2)}\sin(\theta_{j_1}+\theta_{j_2}-2\theta_i) \\ & + \cdots \\ & + \frac{K_D}{D!\langle k^{(D)}\rangle}\sum_{j_1,j_2,\ldots,j_D=1}^{N} M_{ij_1\cdots j_D}^{(D)}\sin\left(\sum_{d=1}^{D}\theta_{j_d}-D\theta_i\right), \quad (1)\end{aligned}$$

where $\theta_i \in [0,2\pi)$ represents the phase of oscillator i and ω_i denotes its natural frequency. The adjacency tensors $M_{ij_1\cdots j_d}^{(d)}$ describe multi-order interactions between oscillators $i, j_1, \ldots, j_d$. For example, $M_{ij}^{(1)} = 1$ if oscillators i and j have a pair-wise (1-hyperedge) interaction, and 0 otherwise; $M_{ijl}^{(2)} = 1$ if oscillators i, j, and l have a three-body (2-hyperedge) interaction, and 0 otherwise. K_d denotes the coupling strengths of d-hyperedge interactions. All interactions are assumed to be unweighted and undirected. The generalized degree of oscillator i at order d, i.e., the number of distinct d-hyperedges that oscillator i is part of, is given by $k_i^{(d)} = \frac{1}{d!}\sum_{j_1,j_2,\ldots,j_d=1}^{N} M_{ij_1\cdots j_d}^{(d)}$, which is normalized by a factor of $d!$ to avoid repeated computations of the same hyperedge,[21] and $\langle k^{(d)}\rangle$ represents the average generalized degree of all oscillators at order d.

To characterize the collective behavior of the ensemble, the order parameter is introduced as follows:[6]

$$R\mathrm{e}^{\mathrm{i}\psi} = \frac{1}{N}\sum_{j=1}^{N}\mathrm{e}^{\mathrm{i}\theta_j}, \quad (2)$$

where R and ψ are the amplitude and argument, respectively. The order parameter R measures the coherence of the oscillator population. $R = 1$ indicates that the oscillators are perfectly synchronous, and the synchronization is progressively lost as R decreases.

3. Optimizing dynamics on hypergraphs

3.1. Generalized Laplacian matrix

In the study presented in Ref. [35], the inscribability of "open triangles" (e.g., the coincidental accumulation of pairwise edges that do not participate in three-body interactions, meaning that only lower-order interactions exist) in simplicial complexes is precluded due to the derivation of their higher-order adjacency tensors from lower-order components within their composite Laplacian matrices. Similarly, due to the inherent limitations of simplicial complexes, structures with higher-order interactions but no direct lower-order interactions are also excluded. Instead of using simplicial complexes, higher-order networks can alternatively be represented by hypergraphs, which offer greater freedom in describing higher-order interactions. Consequently, the introduction of a more generalized Laplacian matrix, which can characterize the interplay between the collective dynamics and the network structure of the dynamical systems on hypergraphs, is warranted. The generalized Laplacian matrix of order d, which considers only d-order interactions, can be defined as[30]

$$L_{ij}^{(d)} = dk_i^{(d)}\delta_{ij} - A_{ij}^{(d)}, \quad (3)$$

where δ_{ij} is the Kronecker delta, and $A_{ij}^{(d)}$ denotes the generalized degree between oscillators i and j at order d,

$$A_{ij}^{(d)} = \frac{1}{(d-1)!}\sum_{j_2,j_3,\ldots,j_d=1}^{N} M_{ijj_2\cdots j_d}^{(d)}, \quad (4)$$

i.e., the number of d-hyperedges shared by i and j.

3.2. Synchronization optimization with the multi-order Laplacian matrix

Synchronization optimization refers to a system being as strongly synchronized as possible. A detailed theoretical analysis framework can be found in Ref. [35]. In the context of a strongly synchronized system, where the phase difference between any two oscillators i and j, denoted as $|\theta_j - \theta_i|$, is sufficiently small (ideally much less than 1), it becomes feasible to linearize the governing equation by utilizing the Laplacian matrix. This linearization simplifies the optimization of the collective behavior into a formula that can be more readily understood and manipulated mathematically,

$$\dot{\boldsymbol{\theta}} = \boldsymbol{\omega} - \boldsymbol{L}^{(\mathrm{mul})}\boldsymbol{\theta}, \tag{5}$$

where $\boldsymbol{L}^{(\mathrm{mul})}$ denotes the multi-order Laplacian matrix, i.e., the weighted sum of the normalized d-order Laplacian matrices,[30]

$$L_{ij}^{(\mathrm{mul})} = \sum_{d=1}^{D} \frac{K_d}{\langle k^{(d)} \rangle} L_{ij}^{(d)}. \tag{6}$$

For convenience, we transition into a rotating reference frame by applying the transformation $\boldsymbol{\theta} \to \boldsymbol{\theta} + \langle \boldsymbol{\omega} \rangle t$, thereby setting the average frequency to zero. By employing the Moore–Penrose pseudoinverse method on the integrated Laplacian, denoted as $\boldsymbol{L}^{(\mathrm{mul})\dagger} = \sum_{j=2}^{N} \lambda_j^{-1} \boldsymbol{v}_j^{(\mathrm{mul})} \boldsymbol{v}_j^{(\mathrm{mul})\mathrm{T}}$, where $0 = \lambda_1^{(\mathrm{mul})} < \lambda_2^{(\mathrm{mul})} \leq \cdots \leq \lambda_N^{(\mathrm{mul})}$ represent the eigenvalues of $\boldsymbol{L}^{(\mathrm{mul})}$ and the corresponding eigenvectors $\{\boldsymbol{v}_j^{(\mathrm{mul})}\}_{j=1}^{N}$ establish an orthonormal framework for $\mathbb{R}^N$, we ascertain the fixed point

$$\boldsymbol{\theta}^* = \boldsymbol{L}^{(\mathrm{mul})\dagger}\boldsymbol{\omega}. \tag{7}$$

By substituting the fixed point into the order parameter R defined in Eq. (2), the degree of synchronization at the fixed point is approximated by $R \approx 1 - \|\boldsymbol{\theta}^*\|^2/(2N)$. Consequently, the synchronization of the collective behavior can be optimized by minimizing the variance of the fixed point, $\|\boldsymbol{\theta}^*\|^2/N$. Given the specified form of $\boldsymbol{L}^{(\mathrm{mul})\dagger}$ and the relation $\|\boldsymbol{\theta}^*\|^2 = \langle \boldsymbol{\theta}^*, \boldsymbol{\theta}^* \rangle$, it is inferred that

$$\frac{\|\boldsymbol{\theta}^*\|^2}{N} = J\left(\boldsymbol{\omega}, \boldsymbol{L}^{(\mathrm{mul})}\right) = \frac{1}{N}\sum_{j=2}^{N} \frac{\left\langle \boldsymbol{v}_j^{(\mathrm{mul})}, \boldsymbol{\omega} \right\rangle^2}{\left(\lambda_j^{(\mathrm{mul})}\right)^2}, \tag{8}$$

where $J\left(\boldsymbol{\omega}, \boldsymbol{L}^{(\mathrm{mul})}\right)$ denotes the SAF.[34,35] Upon analyzing the contributions to SAF, it is observed that each term corresponds to the squared projection of the frequency vector $\boldsymbol{\omega}$ onto an eigenvector $\boldsymbol{v}_j^{(\mathrm{mul})}$, scaled by the inverse square of the associated eigenvalue $\lambda_j^{(\mathrm{mul})}$. To minimize the function, the main idea is to align $\boldsymbol{\omega}$ as closely as possible with the dominant eigenvectors, corresponding to the larger eigenvalues, while orthogonalizing $\boldsymbol{\omega}$ with respect to the subordinate eigenvectors, associated with the smaller eigenvalues.[35] Therefore, when fixing the variance of the frequency vector at σ^2, the optimal configuration is achieved by setting $\boldsymbol{\omega}$ to $\sigma\sqrt{N}\boldsymbol{v}_N^{(\mathrm{mul})}$, where $\boldsymbol{v}_N^{(\mathrm{mul})}$ denotes the most prominent eigenvector.

At the optimal setting of $\boldsymbol{\omega} = \sigma\sqrt{N}\boldsymbol{v}_N^{(\mathrm{mul})}$, the optimal order parameter corresponding to the optimal synchronization is given by $R = 1 - \sigma^2/(\lambda_N^{(\mathrm{mul})})^2$. Therefore, the synchronization limit of the higher-order Kuramoto model on an arbitrary hypergraph depends on the maximum eigenvalue $\lambda_N^{(\mathrm{mul})}$ of the multi-order Laplacian matrix, with a larger maximum eigenvalue $\lambda_N^{(\mathrm{mul})}$ indicating a higher synchronization limit.

3.3. Numerical simulations

For the sake of clarity, in what follows, we illustrate the case of $D = 2$, i.e., the higher-order Kuramoto model with only pairwise and three-body interactions, to validate our theoretical analysis results. The underlying network is configured as a stochastic hypergraph characterized by an average degree $\langle k_1 \rangle$ and an average 2-hyperdegree $\langle k_2 \rangle$. The construction methodology is inspired by that of random simplicial complexes,[45] and the algorithm is proposed as follows: Given N oscillators, every oscillator pair (i, j) is linked by an edge with a probability $p_1 = k_1/(N-1)$; concurrently, every oscillator triplet (i, j, l) is bound by a 2-hyperedge with a probability $p_2 = 2k_2/[(N-1)(N-2)]$.

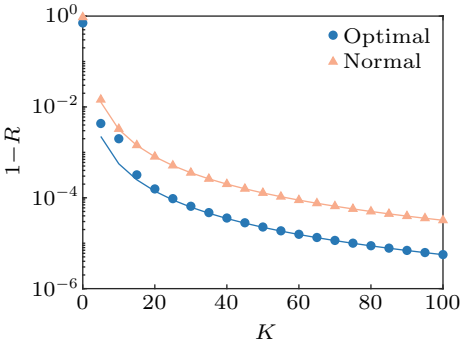


Fig. 1. Optimal synchronization of the higher-order Kuramoto model on a random hypergraph. The synchronization error $1 - R$ vs. the scaled coupling strength K ($K = 2K_1 = 2K_2$) for standard normal distribution (blue circles) and optimal (pink triangles) natural frequencies, respectively. The solid lines are theoretical values from Eq. (8). The network size is $N = 500$, and the average degree and the average 2-hyperdegree are $\langle k_1 \rangle = 20$, $\langle k_2 \rangle = 6$, respectively.

When the scaled coupling strength K ($K = 2K_1 = 2K_2$) is small, synchronization does not occur, as depicted in Fig. 1, likely due to insufficient coupling to achieve strong synchronization. However, at larger values of K, the proposed method in hypergraphs is validated, with the synchronization error $1 - R$ reduced by an order of magnitude and a strong agreement between theoretical and simulated results. Further experiments confirm the algorithm's applicability across hypergraph sizes and reveal the distribution of the optimal natural frequency in a random case (see Figs. S1 and S2).

4. Optimizing topology for synchronization

4.1. Component contributions of hyperedges to eigenvalues

As proved above, the upper bound of synchronous behavior for the higher-order Kuramoto model on hypergraphs is governed by the maximum eigenvalue λ_N of the multi-order Laplacian matrix $\boldsymbol{L}^{(\mathrm{mul})}$, which is entirely determined by the topological structure of the hypergraph. Thus, modifying the network topology to enlarge the maximum eigenvalue can effectively raise the upper bound, leading to optimal network synchronization and a broader eigenvalue spectrum.

In practical scenarios, the total resource availability is typically constrained, necessitating the optimization of resource allocation to maximize overall benefits. Consequently, efforts to increase the maximum eigenvalue of the multi-order Laplacian matrix must focus on redistributing hyperedges while maintaining a fixed total number of hyperedges. Here, it is assumed that the quantity of hyperedges at each order remains constant.

For a uniform hypergraph that contains only d-hyperedges, the relationship between the d-order Laplacian matrix $\boldsymbol{L}^{(d)}$ and the normalized eigenvector $\boldsymbol{v}_m^{(d)}$ corresponding to the mth eigenvalue $\lambda_m^{(d)}$ ($m=1,2,\ldots,N$) (where eigenvalues $\lambda_1^{(d)},\lambda_2^{(d)},\ldots,\lambda_N^{(d)}$ are assumed to be sorted in ascending order unless otherwise stated) can be obtained by the following eigen equation:

$$\boldsymbol{L}^{(d)}\boldsymbol{v}_m^{(d)}=\lambda_m^{(d)}\boldsymbol{v}_m^{(d)}. \tag{9}$$

Multiplying both sides of the above equation by $\boldsymbol{v}_m^{(d)\mathrm{T}}$ yields

$$\boldsymbol{v}_m^{(d)\mathrm{T}}\boldsymbol{L}^{(d)}\boldsymbol{v}_m^{(d)}=\lambda_m^{(d)}\boldsymbol{v}_m^{(d)\mathrm{T}}\boldsymbol{v}_m^{(d)}=\lambda_m^{(d)}\|\boldsymbol{v}_m^{(d)}\|^2=\lambda_m^{(d)}, \tag{10}$$

where T is the matrix transpose operator. Hence, the d-order eigenvalues $\lambda_m^{(d)}$ ($m=1,2,\ldots,N$, i.e., the d-order eigenvalue spectrum) can be expressed as a quantity derived from the d-order Laplacian matrix.

The key to maximizing $\lambda_N^{(d)}$ lies in decomposing the contributions of all hyperedges to the maximum eigenvalue. By definition, the d-order Laplacian matrix can be expressed as a linear combination of d-hyperedge components. Concretely, we first define the component matrix of each d-hyperedge $e=\{i_1,i_2,\ldots,i_{d+1}\}$ in the multi-order Laplacian matrix as

$$L_{ij}^{(e)}=\begin{cases} d, & \text{if } i=j \text{ and } i,j\in e,\\ -1, & \text{if } i\neq j \text{ and } i,j\in e,\\ 0, & \text{otherwise.}\end{cases} \tag{11}$$

Then, the d-order Laplacian matrix can be represented as the sum of the component matrices of all d-hyperedges,

$$\boldsymbol{L}^{(d)}=\sum_{e\in E_d}\boldsymbol{L}^{(e)}, \tag{12}$$

where E_d denotes the set of d-hyperedges. Figure 2(a) presents an example of a hypergraph with five oscillators, where two 2-hyperedges correspond to the two green matrices in Fig. 2(b). The second-order Laplacian matrix corresponds to the sum of these two component matrices.

Moreover, the eigenvalues of the d-order Laplacian matrix can be expressed as

$$\lambda_m^{(d)}=\sum_{e\in E_d}\boldsymbol{v}_m^{(d)\mathrm{T}}\boldsymbol{L}^{(e)}\boldsymbol{v}_m^{(d)}=\sum_{e\in E_d}\lambda_m^{(e)}, \tag{13}$$

where $m=1,2,\ldots,N$, and $\lambda_m^{(e)}$ represents the mth eigenvalue of the component matrix of the d-hyperedge e.

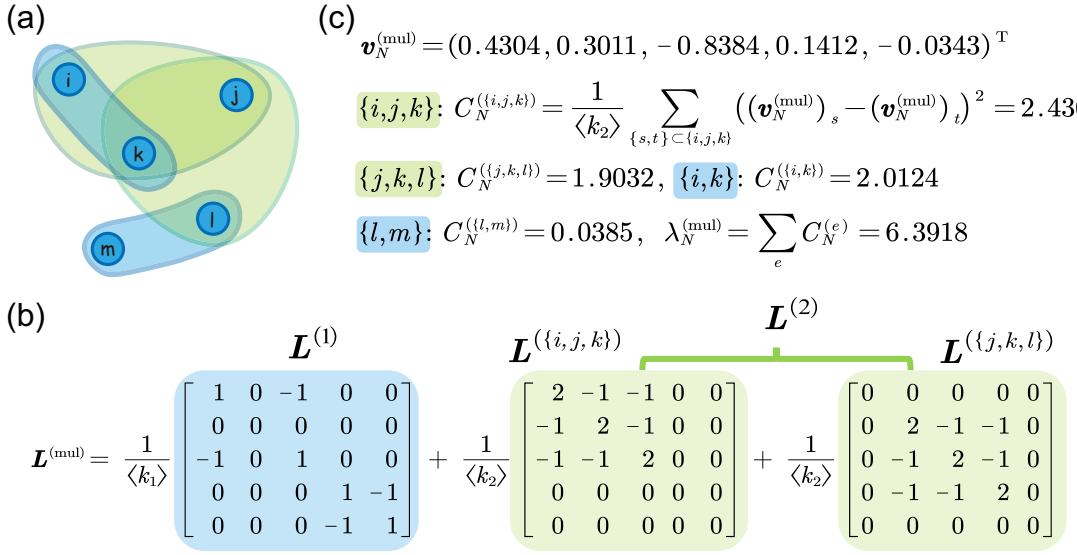


Fig. 2. Procedure for calculating the contribution of hyperedges to the eigenvalues. (a) Illustration of a hypergraph with five nodes, including two 1-hyperedges (blue) and two 2-hyperedges (green). (b) The multi-order Laplacian matrix is obtained as a weighted sum of the first-order Laplacian matrix (blue matrix) and the second-order Laplacian matrix (the sum of the two green matrices, each of which corresponds to the component matrix of a 2-hyperedge in panel (a)). $\langle k_d\rangle$ is the average generalized degree of order d. (c) Contribution of each hyperedge computed according to Eq. (16).

For the multi-order Laplacian matrix, we note that $\gamma_d \equiv K_d/\langle k^{(d)}\rangle$. Then, the multi-order Laplacian can be expressed as

$$\boldsymbol{L}^{(\mathrm{mul})} = \sum_{d=1}^{D} \gamma_d \boldsymbol{L}^{(d)} = \sum_{d=1}^{D} \sum_{e\in E_d} \gamma_d \boldsymbol{L}^{(e)}, \tag{14}$$

as shown in Figs. 2(a) and 2(b) ($K_i = 1$). The corresponding eigenvalues (i.e., eigenvalue spectrum) are obtained by

$$\begin{aligned}\lambda_m^{(\mathrm{mul})} &= \boldsymbol{v}_m^{(\mathrm{mul})\mathrm{T}} \boldsymbol{L}^{(\mathrm{mul})} \boldsymbol{v}_m^{(\mathrm{mul})} \\ &= \boldsymbol{v}_m^{(\mathrm{mul})\mathrm{T}} \left(\sum_{d=1}^{D} \sum_{e\in E_d} \gamma_d \boldsymbol{L}^{(e)} \right) \boldsymbol{v}_m^{(\mathrm{mul})} \\ &= \sum_{d=1}^{D} \gamma_d \sum_{e\in E_d} \boldsymbol{v}_m^{(\mathrm{mul})\mathrm{T}} \boldsymbol{L}^{(e)} \boldsymbol{v}_m^{(\mathrm{mul})},\end{aligned} \tag{15}$$

where $m = 1, 2, \ldots, N$.

The above analysis indicates that the eigenvalues of the multi-order Laplacian matrix for a hypergraph can be decomposed into a weighted sum of contributions from the component matrices of each hyperedge and the corresponding eigenvector of the multi-order Laplacian matrix. Therefore, we define the contribution of each hyperedge e to the mth eigenvalue of the multi-order Laplacian matrix as

$$\begin{aligned}C_m^{(e)} &\equiv \gamma_{d_e} \boldsymbol{v}_m^{(\mathrm{mul})\mathrm{T}} \boldsymbol{L}^{(e)} \boldsymbol{v}_m^{(\mathrm{mul})} \\ &= \gamma_{d_e} \sum_{\{i,j\}\subset e} \left[\left(\boldsymbol{v}_m^{(\mathrm{mul})}\right)_i - \left(\boldsymbol{v}_m^{(\mathrm{mul})}\right)_j \right]^2,\end{aligned} \tag{16}$$

where d_e denotes the order of hyperedge e; $(\boldsymbol{v}_m^{(\mathrm{mul})})_i$ and $(\boldsymbol{v}_m^{(\mathrm{mul})})_j$ are the ith and jth components of the mth eigenvector $\boldsymbol{v}_m^{(\mathrm{mul})}$, respectively. This indicates that the contribution of a hyperedge to the eigenvalue is essentially the sum of the contributions from each pair of oscillators within the hyperedge. Finally, the eigenvalue spectrum of the multi-order Laplacian matrix for an arbitrary hypergraph is obtained as

$$\lambda_m^{(\mathrm{mul})} = \sum_e C_m^{(e)}, \tag{17}$$

with $m = 1, 2, \ldots, N$ (Fig. 2(c)). In particular, when the hypergraph consists solely of d-hyperedges, the mth eigenvalue $\lambda_m^{(\mathrm{mul})}$ of the multi-order Laplacian matrix reduces to $\lambda_m^{(d)}$, with $C_m^{(e)} = \gamma_d \boldsymbol{v}_m^{(d)\mathrm{T}} \boldsymbol{L}^{(e)} \boldsymbol{v}_m^{(d)}$.

4.2. Eigenvalue-based topological modification algorithms

After determining the contribution of each hyperedge to the eigenvalue of the multi-order Laplacian matrix for a hypergraph, a natural strategy is to remove hyperedges with lower contributions and incorporate those with higher contributions to enhance the maximum eigenvalue $\lambda_N^{(\mathrm{mul})}$, ultimately leading to an improvement in the degree of synchronization between oscillators. As the operations of removal and addition are restricted to hyperedges of the same order, the average generalized degree of the network remains constant.

Taking the modification of d-hyperedges as an example, the algorithm proceeds as follows: First, compute the eigenvector $\boldsymbol{v}_N^{(\mathrm{mul})}$ corresponding to the maximum eigenvalue $\lambda_N^{(\mathrm{mul})}$ of the multi-order Laplacian matrix $\boldsymbol{L}^{(\mathrm{mul})}$. Then, traverse through all d-hyperedges f to calculate their contributions $C_N^{(f)}$ to the maximum eigenvalue $\lambda_N^{(\mathrm{mul})}$ and randomly delete one hyperedge e from the set of n d-hyperedges with the smallest contributions (i.e., the last n hyperedges when all contributions are arranged in descending order). Next, iterate over all possible d-hyperedges f' to calculate their potential contributions $C_N^{(f')}$ and randomly add one hyperedge e' from the set of n d-hyperedges with the largest potential contributions (i.e., the first n hyperedges when all contributions are arranged in descending order). Finally, check whether the maximum eigenvalue $\lambda_N^{(\mathrm{mul})}$ increases: if it does, accept the change; otherwise, accept it with a certain probability P. Repeat the above steps until a termination condition is met (e.g., a specified number of iterations or reaching a predefined threshold). The pseudocode for the algorithm is displayed in Algorithm 1.

Algorithm 1: Optimize hypergraph to increase $\lambda_N^{(\mathrm{mul})}$.

Input: Hypergraph H, d-hyperedges set E_d, number of candidate hyperedges n, accept probability P, termination condition.
Output: Optimized hypergraph H, Optimized d-hyperedges set E_d.
Initialize H, compute $\boldsymbol{L}^{(\mathrm{mul})}, \boldsymbol{v}_N^{(\mathrm{mul})}$ and possible d-hyperedge set E_d'
Compute the maximum eigenvalue $\lambda_N^{(\mathrm{mul})}$ of $\boldsymbol{L}^{(\mathrm{mul})}$
while termination condition not met **do**
    // Step 1: Delete d-hyperedges
    for each d-hyperedge $e \in E_d$ **do**
        Compute the contribution $C_N^{(e)}$
    end for
    Select n d-hyperedges with the smallest contribution
    Randomly remove one d-hyperedge from the selected set
    // Step 2: Add d-hyperedges
    for each possible d-hyperedge $e' \in E_d'$ **do**
        Compute the potential contribution $C_N^{(e')}$
    end for
    Select n possible d-hyperedges with the largest potential contribution
    Randomly add one d-hyperedge from the selected set
    // Step 3: Validate changes
    Recompute $\boldsymbol{L}^{(\mathrm{mul})'}, \boldsymbol{v}_N^{(\mathrm{mul})'}$ and $\lambda_N^{(\mathrm{mul})'}$ for the modified hypergraph
    if $\lambda_N^{(\mathrm{mul})'} \geq \lambda_N^{(\mathrm{mul})}$ **then**
        Accept the modification and update parameters
    else
        Accept the modification with probability P
        Update P
    end if
end while
Return: Optimized hypergraph H, Optimized d-hyperedges set E_d.

The complexity of the algorithm primarily lies in calculating the contributions of all already existing hyperedges and

potential hyperedges. Suppose there are N oscillators, M_1 existing d-hyperedges, and M_2 possible d-hyperedges. Clearly, the union of M_1 and M_2 represents all $(d+1)$-tuples. According to Eq. (16), computing the contribution for each hyperedge requires $O(d^2)$. Therefore, the algorithmic complexity for one iteration is approximately $O(\binom{N}{d+1}d^2)$. When the termination condition is set to a specified number of iterations C_{iter}, the overall complexity of the algorithm is approximately $O(C_{\text{iter}}\binom{N}{d+1}d^2)$. Under specific conditions, such as simplicial complexes or when the number of potential hyperedges is limited, this complexity can be significantly reduced.

4.3. Results of topological modification algorithms on synthetic networks

Figure 3 illustrates an example of the topology modification algorithm applied to a random hypergraph with $D=2$. The networks are randomly generated by specifying average degrees. The topology modification algorithm modifies the distribution of 2-hyperedges while keeping the 1-hyperedges unchanged. The maximum number of iterations is $T=500$, and the acceptance probability is

$$P=\begin{cases} \mathrm{e}^{\left(\lambda_N^{(\mathrm{mul})'}-\lambda_N^{(\mathrm{mul})}\right)/(T-t)}, & \lambda_N^{(\mathrm{mul})'}<\lambda_N^{(\mathrm{mul})}, \\ 1, & \lambda_N^{(\mathrm{mul})'}\geq\lambda_N^{(\mathrm{mul})}, \end{cases} \tag{18}$$

where $\lambda_N^{(\mathrm{mul})}$ and $\lambda_N^{(\mathrm{mul})'}$ are the maximum eigenvalues of the multi-order Laplacian matrices $\boldsymbol{L}^{(\mathrm{mul})}$ before and after the removal and addition of a hyperedge, respectively, and t is the current iteration step.

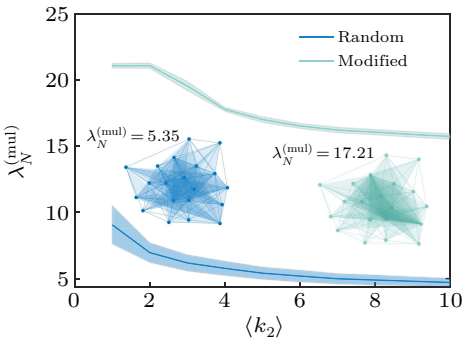


Fig. 3. Changes in hyperedge distribution and the maximum eigenvalue of the multi-order Laplacian matrix before and after topological modification. Fixed $\langle k_1\rangle=10$, with simulation results for random hypergraph networks with different $\langle k_2\rangle$. Blue and green represent the hyperedge distributions before and after optimization by the modification algorithm, respectively. Solid lines and shaded areas correspond to the average and variance of results over 100 simulations. The subplot illustrates a visual representation of a network with $\langle k_2\rangle=5$ before and after modification.

The results indicate a substantial increase in the maximum eigenvalue for the modified hypergraph, accompanied by minimal variance, thereby confirming both the effectiveness and stability of the algorithm. Following the modification, the distribution of 2-hyperedges becomes notably more heterogeneous, exhibiting a radial pattern around a few central hyperedges, in contrast to the prior random distribution. This outcome is consistent with the relationship between the maximum eigenvalue of the Laplacian matrix and the generalized degree as follows.

By leveraging the Rayleigh quotient and the properties of weighted Laplacians,[46] the largest eigenvalue of the hypergraph can be estimated to fall within the following interval:

$$k_{\max}^{(\mathrm{mul})}\leq\lambda_N^{(\mathrm{mul})}<k_{\max}^{(\mathrm{mul})}+k_{\mathrm{secondmax}}^{(\mathrm{mul})}, \tag{19}$$

with

$$k_{\max}^{(\mathrm{mul})}=\max\left\{k_i^{(\mathrm{mul})},i=1,2,\ldots,N\right\},$$
$$k_{\mathrm{secondmax}}^{(\mathrm{mul})}=\max\left\{k_i^{(\mathrm{mul})}\mid k_i^{(\mathrm{mul})}<k_{\max}^{(\mathrm{mul})},\ \ i=1,2,\ldots,N\right\},$$

where $k_i^{(\mathrm{mul})}$ denotes the composite degree, corresponding to the i-th diagonal element of the multi-order Laplacian matrix,

$$k_i^{(\mathrm{mul})}=\frac{K_1}{\langle k^{(1)}\rangle}k_i^{(1)}+\frac{K_2}{\langle k^{(2)}\rangle}2k_i^{(2)}=L_{ii}^{(\mathrm{mul})}. \tag{20}$$

The maximum eigenvalue of the network's multi-order Laplacian matrix is closely related to the network's composite degree. Therefore, networks characterized by extremely large composite degrees (e.g., hubs) typically exhibit a larger expected maximum eigenvalue $\lambda_N^{(\mathrm{mul})}$. This insight underscores the notion that networks with stronger heterogeneity tend to have superior optimization potential.

5. Simulation on real datasets

Furthermore, we validate our optimization algorithm and topology modification strategy on real-world datasets. The datasets include interaction information between individuals from schools, workplaces, and academic conferences (see Fig. S3 for results on synthetic networks). Using the reconstruction method defined in Ref. [45], we construct a simplicial network from real interaction data. The topology modification method is applied to reconstruct the three-body interactions. We simulate these three networks using both random natural frequencies and optimal natural frequencies, with the results presented in Fig. 4. The schematic of the network topology is shown in Figs. 4(a)–4(c), with the network before and after modification represented in blue and green, respectively. The modified network exhibits greater heterogeneity, displaying a hub-like structure centered around a few central oscillators or hyperedges, consistent with the previous conclusion. In Figs. 4(d)–4(f), the optimal natural frequencies significantly enhance synchronization across all social networks, closely aligning with theoretical values. Moreover, the modified network achieves a higher synchronization upper bound compared to that of three-body interactions

derived from real-world data. Before frequency optimization, the modified topology demonstrates lower synchronization, while after optimization, synchronization improves significantly. This indicates that the topology modification strategy expands the state space of the system, while the optimized natural frequency positions the system in its optimal state. In summary, in uncontrolled social systems, uniform interactions facilitate faster message synchronization, while in regulated systems, the presence of core nodes or links (such as influential media or leaders) can further enhance synchronization.

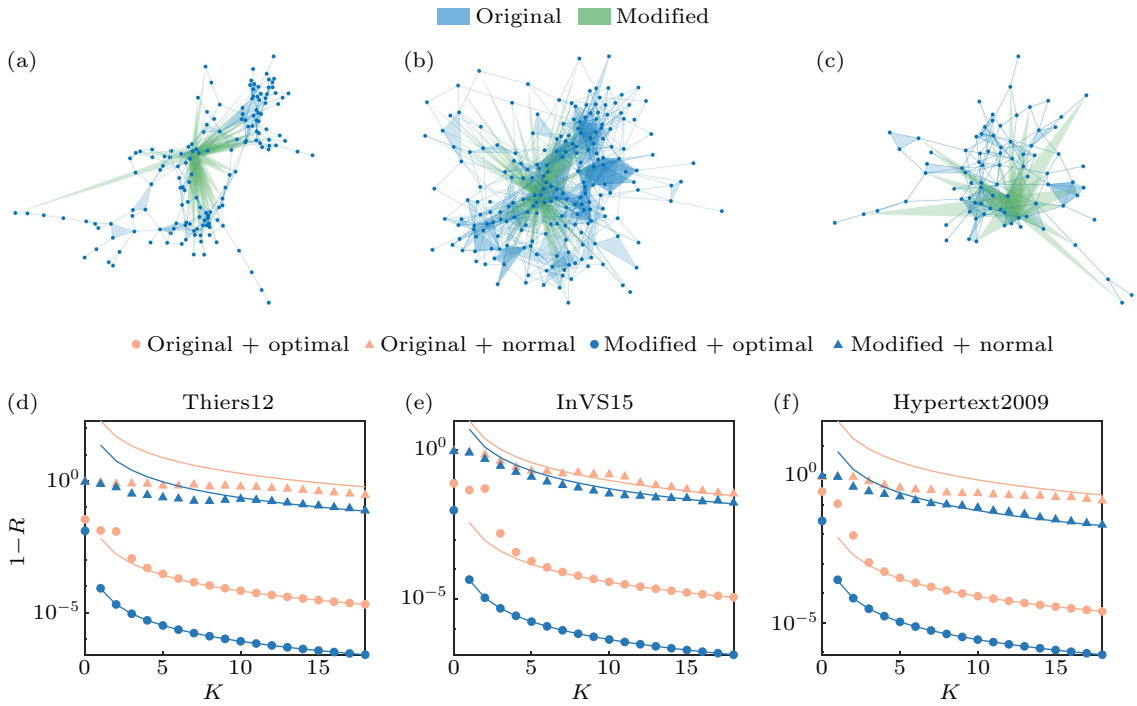


Fig. 4. Illustration of topology modification and simulation experiments on three real social networks. (a)–(c) Schematic of three-body interactions reconstructed from real interactions (blue) and after topology modification (green) across three social networks: schools (Thiers12), workplaces (InVS15), and academic conferences (Hypertext2009). (d)–(f) Numerical simulation results before and after topology modification and natural frequency optimization, showing the synchronization error $1-R$ vs. the scaled coupling strength K ($K = 2K_1 = 2K_2$) for different combinations. The solid lines represent theoretical values from Eq. (8).

6. Conclusion

This paper presents synchronization optimization strategies for the higher-order Kuramoto model on hypergraphs, including the calculation of the optimal natural frequency distribution and a topology modification algorithm. The internal mechanism is deeply analyzed from a microscopic perspective.

First, based on the multi-order Laplacian matrix of hypergraphs, we expand the synchronization optimization strategy proposed by Skardal, which was originally based on simplicial complexes, and extend it to more general hypergraphs of arbitrary order. This modification overcomes the limitations of the original approach, eliminating the effect of dependence between structures of different orders on the results. Through theoretical derivation, we conclude that the upper bound of synchronous behavior for the higher-order Kuramoto model on hypergraphs is determined by the maximum eigenvalue of the multi-order Laplacian matrix, and the optimal natural frequency distribution depends on its corresponding eigenvector. The larger the maximum eigenvalue, the higher the upper bound.

Next, we propose a hypergraph topology modification algorithm that effectively adjusts the eigenvalues of the multi-order Laplacian matrix, thereby enhancing the upper bound of synchronous behavior. Using the linear superposition property of the multi-order Laplacian matrix, we decompose the contribution of each hyperedge to the eigenvalue. The hyperedges with larger contributions are iteratively used to replace those with smaller contributions, leading to an increase in the eigenvalue. The results demonstrate that the heterogeneous hypergraph has larger maximum eigenvalues of the multi-order Laplacian matrix and higher upper bounds of synchronous behavior, even though it exhibits lower synchronization expectation when non-optimized.

The proposed optimization strategy and topology modification algorithm are validated on three real-world datasets. The results show that natural frequency optimization effectively improves synchronization, regardless of the topology. Additionally, the modified topology achieves better optimization, with a higher degree of synchronization compared to the three-body interactions reconstructed from the real data. The optimized topologies generally exhibit heterogeneous distri-

butions, leading to higher upper limits of synchronous behavior and lower synchronization expectations. This indicates that homogeneous interaction systems are better synchronized without the need for additional interventions, while heterogeneous interaction systems tend to show higher extremes under certain regulatory conditions.

The topology modification algorithm proposed in this paper is highly scalable and capable of tuning any eigenvalue of the multi-order Laplacian matrix of a hypergraph (or simplicial complex) of arbitrary order. For instance, tuning the eigenvalues of a simplex network can be accomplished by simply adjusting the range of selected hyperedges within the simplex. The well-known Fiedler value λ_2 can be modified by altering the eigenvectors in the contribution formula, thus enabling modifications to network stability-related properties.[47]

Acknowledgments

Project supported by the National Natural Science Foundation of China (Grant Nos. 12247153, T2293771, and 12247101), the Zhejiang Provincial Natural Science Foundation of China (Grant No. LTGY24A050002), the Sichuan Science and Technology Program (Grant Nos. 2024NSFSC1364 and 2023NSFSC1919), the Project of Huzhou Science and Technology Bureau (Grant No. 2022YZ29), the UESTCYDRI research start-up (Grant No. U03210066), and the New Cornerstone Science Foundation through the Xplorer Prize.

References

[1] Strogatz S H 2003 *Sync: The Emerging Science of Spontaneous Order* (New York, Hyperion)
[2] Fell J and Axmacher N 2011 *Nat. Rev. Neurosci.* **12** 105
[3] Wang C Y, Zhang J Q, Wu Z X and Guan J Y 2021 *Phys. Rev. E* **103** 022312
[4] Pluchino A, Latora V and Rapisarda A 2005 *Int. J. Mod. Phys. C* **16** 515
[5] Shahal S, Wurzberg A, Sibony I, Duadi H, Shniderman E, Weymouth D, Davidson N and Fridman M 2020 *Nat. Commun.* **11** 3854
[6] Acebrón J A, Bonilla L L, Pérez Vicente C J, Ritort F and Spigler R 2005 *Rev. Mod. Phys.* **77** 137
[7] Rohden M, Sorge A, Timme M and Witthaut D 2012 *Phys. Rev. Lett.* **109** 064101
[8] Skardal P S and Arenas A 2015 *Sci. Adv.* **1** e1500339
[9] Albert R and Barabási A L 2002 *Rev. Mod. Phys.* **74** 47
[10] Boccaletti S, Latora V, Moreno Y, Chavez M and Hwang D U 2006 *Phys. Rep.* **424** 175
[11] Newman M E J 2018 *Networks: An Introduction*, 2nd ed (New York: Oxford University Press)
[12] Arenas A, Díaz-Guilera A, Kurths J, Moreno Y and Zhou C 2008 *Phys. Rep.* **469** 93
[13] Rodrigues F A, Peron T K D, Ji P and Kurths J 2016 *Phys. Rep.* **610** 1
[14] Wu X, Wu X, Wang C Y, Mao B, Lu J, Lü J, Zhang Y C and Lü L 2024 *Phys. Rep.* **1060** 1
[15] Duolan, Xiang L and Chen G 2023 *Chin. Phys. B* **32** 060502
[16] Benson A R, Gleich D F and Leskovec J 2016 *Science* **353** 163
[17] Battiston F, Amico E, Barrat A, Bianconi G, Ferraz De Arruda G, Franceschiello B, Iacopini I, Kéfi S, Latora V, Moreno Y, Murray M M, Peixoto T P, Vaccarino F and Petri G 2021 *Nat. Phys.* **17** 1093
[18] Zheng H X, Miao S Y and Gu C G 2024 *Chin. Phys. B* **33** 058401
[19] Salnikov V, Cassese D and Lambiotte R 2019 *Eur. J. Phys.* **40** 014001
[20] Battiston F, Cencetti G, Iacopini I, Latora V, Lucas M, Patania A, Young J G and Petri G 2020 *Phys. Rep.* **874** 1
[21] Bianconi G 2021 *Higher-Order Networks* (Cambridge: Cambridge University Press)
[22] Liu B, Zeng Y J, Yang R M and Lü L Y 2024 *Acta Phys. Sin.* **73** 128901 (in Chinese)
[23] Tanaka T and Aoyagi T 2011 *Phys. Rev. Lett.* **106** 224101
[24] Skardal P S and Arenas A 2019 *Phys. Rev. Lett.* **122** 248301
[25] Berner R, Vock S, Schöll E and Yanchuk S 2021 *Phys. Rev. Lett.* **126** 028301
[26] Kovalenko K, Dai X, Alfaro-Bittner K, Raigorodskii A M, Perc M and Boccaletti S 2021 *Phys. Rev. Lett.* **127** 258301
[27] Zhang Y, Skardal P S, Battiston F, Petri G and Lucas M 2024 *Sci. Adv.* **10** eado8049
[28] Wu Y, Yu H, Zheng Z and Xu C 2024 *Chin. Phys. B* **33** 040504
[29] Skardal P S and Arenas A 2020 *Commun. Phys.* **3** 218
[30] Lucas M, Cencetti G and Battiston F 2020 *Phys. Rev. Res.* **2** 033410
[31] Kundu S and Ghosh D 2022 *Phys. Rev. E* **105** L042202
[32] Ji B Y, Wang C Y and Lü L 2025 *New J. Phys.* **27** 043012
[33] Zheng Z 2019 *Emergence dynamics in complex systems: From synchronization to collective transport* (Beijing: Science Publishing House) (in Chinese)
[34] Skardal P S, Taylor D and Sun J 2014 *Phys. Rev. Lett.* **113** 144101
[35] Skardal P S, Arola-Fernández L, Taylor D and Arenas A 2021 *Phys. Rev. Res.* **3** 043193
[36] Wang X F and Chen G 2002 *IEEE Trans. Circuits Syst. I* **49** 54
[37] Restrepo J G, Ott E and Hunt B R 2005 *Phys. Rev. E* **71** 036151
[38] Gómez-Gardeñes J and Moreno Y 2006 *Phys. Rev. E* **73** 056124
[39] Gómez-Gardeñes J and Moreno Y 2011 *Phys. Rev. Lett.* **106** 128701
[40] Hart J D, Zhang Y, Roy R and Motter A E 2019 *Phys. Rev. Lett.* **122** 058301
[41] Chen W, Gao J, Lan Y and Xiao J 2022 *Phys. Rev. E* **105** 044302
[42] Hossein Ghorban S, Hesaam B and Sarbazi-Azad H 2022 *J. Stat. Mech.* **2022** 113404
[43] Tang Y, Shi D and Lü L 2022 *Commun. Phys.* **5** 96
[44] Kuramoto Y 1984 *Chemical Oscillations, Waves, and Turbulence* (Berlin, Heidelberg: Springer)
[45] Wang H, Ma C, Chen H S, Lai Y C and Zhang H F 2022 *Nat. Commun.* **13** 3043
[46] Das K C and Bapat R 2005 *Linear Algebra Appl.* **409** 153
[47] Gambuzza L V, Di Patti F, Gallo L, Lepri S, Romance M, Criado R, Frasca M, Latora V and Boccaletti S 2021 *Nat. Commun.* **12** 1255